Astron. Astrophys. 335, 500–509 (1998)

ASTRONOMY AND ASTROPHYSICS

The nature of the magnetic belt in M31

D. Moss[1], **A. Shukurov**[2], **D.D. Sokoloff**[3], **E.M. Berkhuijsen**[4], **and R. Beck**[4]

[1] Department of Mathematics, University of Manchester, Manchester, M13 9PL, UK
[2] Department of Mathematics, University of Newcastle, Newcastle upon Tyne NE1 7RU, UK
[3] Physics Department, Moscow University, Moscow 119899, Russia
[4] Max-Planck-Institut für Radioastronomie, Auf dem Hügel 69, D-53121 Bonn, Germany

Received 19 January 1998 / Accepted 30 March 1998

Abstract. The most conspicuous feature of the large-scale magnetic field in the Andromeda nebula (M31) is a magnetic belt centred at a galacto-centric radius of about $10\,\mathrm{kpc}$. We suggest a nonlinear dynamo model for M31, which associates this belt with the gas density profile as well as with the kinematic parameters of M31. Our model is based on the observed density profile and vertical structure of the gas disc of M31, and on a recent rotation curve. The traditional explanation of the belt in kinematic dynamo theory was connected with a double-peaked form of the rotation curve of M31. We show that this explanation fails with recent determinations of the rotation curve of M31. Furthermore, it is unsatisfactory because it underestimates, even in the kinematic (linear) regime, the interplay of magnetic fields generated at different galacto-centric radii.

Our model predicts an extended belt of magnetic field between 7 and $12\,\mathrm{kpc}$ radius, in accordance with observations. However, our models typically also have another maximum of the regular magnetic field between 2 and $6\,\mathrm{kpc}$ radius which is not obvious in the synchrotron emission. We discuss possible reasons why it could avoid detection if it is real, and suggest a search for the field in this region, e.g. via Faraday rotation of polarized radio sources behind M31.

A further generic feature of our models is that the scale height of the regular magnetic field is significantly larger than that of the gas, and has a steeper increase with galacto-centric radius. This can be important, e.g., for cosmic ray confinement and vertical gas balance.

Key words: magnetic fields – MHD – galaxies: ISM – galaxies: magnetic fields – galaxies: individual: M31 – radio continuum: galaxies

1. Introduction

The magnetic field in the Andromeda nebula (M31, NGC 224) has been studied in considerable detail both observationally and theoretically. Observations of the nonthermal radio emission between 408 MHz and 4750 MHz show that this emission, and hence also the magnetic field, is most pronounced within about 1 kpc from the centre and within a belt or 'ring' at galacto-centric radius $r \simeq 10$ kpc with a marked minimum between these areas (Pooley 1969, Berkhuijsen 1977, Berkhuijsen et al. 1983, Beck 1982, Beck & Gräve 1982, Beck et al. 1980, 1989, 1996, 1998). The emission belt has a full width to half maximum of about 5 kpc in total intensity and consists of several tightly wound spiral arms (Beck et al. 1998) that are also bright in Hα (Devereux et al. 1994), H I (Brinks & Shane 1984), CO (Dame et al. 1993) and far-infrared (Xu & Helou 1994; see also Xu & Helou 1996). The thermal radio emission also peaks in the belt (Beck & Gräve 1982).

The properties of the magnetic field in M31 were studied by Beck (1982), using radio polarization observations at $\lambda 11.1$ cm. In case of equipartition between the energy densities of cosmic rays and the total magnetic field, the field is concentrated in the $10\,\mathrm{kpc}$ belt with a strength of typically $5\,\mu$G for the total and $3\,\mu$G for the regular field. The field orientation is mainly along the belt without large-scale reversals between 7 and $16\,\mathrm{kpc}$ radius. The asymmetric distribution of the polarized emission and Faraday rotation with respect to the minor axis imply that magnetic lines are, on average, inclined to the circumference of the belt by an angle of about 10°. This structure has been confirmed by very recent results at $\lambda 6$ cm by Berkhuijsen, Beck & Hoernes (in prep.).

It should be stressed that, although the strength of the large-scale magnetic field is concentrated within a belt, the field is not azimuthal, but has a spiral shape. From the observation of polarization angles at $\lambda 11.1$ cm the pitch angles and their 2-σ errors were estimated as $p = -18^\circ \pm 8^\circ$ at $r =$ 7–10 kpc and $p = -8^\circ \pm 7^\circ$ at $r =$ 10–13 kpc (Ruzmaikin et al. 1990). From the phase shift of the variation of Faraday rotation measures with azimuthal angle in the plane of M31, Beck (1982) estimated the pitch angle of the field and the 3-σ errors as $p = -17^\circ \pm 3^\circ$ at $r =$ 7–10 kpc, $p = -8.5^\circ \pm 2^\circ$ at $r =$ 10–13 kpc, and $p = -7^\circ \pm 3^\circ$ at $r =$ 13–16 kpc.

The recent high-resolution VLA/Effelsberg survey of M31 (Beck et al. 1998) allows the location of the minimum of the $\lambda 20$ cm emission (which is mainly of synchrotron origin) at a galactocentric radius of about 4 kpc. The average intensity I of the total emission is about 4 times smaller there than at the maximum of the belt. The true minimum is somewhat deeper

Send offprint requests to: D. Moss

due to averaging of data in concentric rings. As $I \propto n_e B^2$, this would mean a total field with strength less than half that in the belt, or a density n_e of cosmic ray electrons that is lower by a factor of four or more.

An explanation of the magnetic field morphology in M31 generally accepted so far was offered by the galactic dynamo model of Ruzmaikin & Shukurov (1981) and Ruzmaikin et al. (1985). Their kinematic $\alpha\omega$-dynamo model for M31 was based on the rotation curves of Rubin & Ford (1970) and Roberts & Whitehurst (1975), which have a well-pronounced double-peaked form. Subsequent refinements of the dynamo model (Baryshnikova et al. 1987, Krasheninnikova et al. 1989; see Ruzmaikin et al. 1988 for a review) used the rotation curves of Deharveng & Pellet (1975) and Haud (1981) which have similar forms. With these rotation curves, the radial gradient of the angular velocity of the galactic rotation is positive near $r = 6\,\mathrm{kpc}$, so that the dynamo does not maintain a large-scale magnetic field in a ring between about 2 and $7\,\mathrm{kpc}$. The dynamo action also ceases at $r \gtrsim 20\,\mathrm{kpc}$. As a result, there are two separate families of kinematic eigenfunctions of the $\alpha\omega$-dynamo which are confined to $0 < r \lesssim 2\,\mathrm{kpc}$ and $7 \lesssim r \lesssim 20\,\mathrm{kpc}$, respectively, with their maxima near the centre and at about $10\,\mathrm{kpc}$. As the radial separation of the two growing eigenmodes was larger than the magnetic diffusion length scale, this was believed to explain the magnetic ring in M31.

In this paper we reconsider this explanation for the following reasons. Firstly, Kent (1989) and Braun (1991) obtained new rotation curves for M31 in which the double peak of the rotation curve is significantly less pronounced, if present at all. Secondly, we propose a considerably more advanced galactic dynamo model based on direct nonlinear simulations of the $\alpha^2\omega$-dynamo in a galactic disc (possibly surrounded by an extended halo).

Briefly, our results are as follows. With the new rotation curve, there are no longer two separate families of kinematic dynamo eigenfunctions separated by a gap in radius. Therefore, there is no ring-like magnetic structure in M31 in the kinematic dynamo regime (i.e. before the field is strong enough for any dynamical feedback onto the dynamo to become important). Moreover, even with the old rotation curve and even at the kinematic stage, the gap in the radial distribution of the magnetic field would be smeared by the outward propagation of the central field which grows faster than that in the outer ring (Moss et al. 1998), This competition between the two families of eigenfunctions was underestimated in the earlier models. The new dynamo model for M31 presented here can reproduce the magnetic belt, but emphasizes the importance of nonlinear dynamo effects, so that the steady-state radial distribution of the large-scale magnetic field is controlled by the gas density profile as well as by the kinematic parameters of the galaxy.

The plan of the paper is as follows. In Sect. 2 we briefly discuss the relevant observational data for the galaxy M31, in Sect. 3 we describe our model of the galaxy and its dynamo, and in Sect. 4 we present our results which are further discussed in Sect. 7.

2. The physical parameters of M31

Interstellar magnetic fields are tied to the diffuse ionized gas which is distributed in a more or less thin disc (Dettmar 1992). This component of the interstellar medium is hard to observe and dynamo models for external galaxies often rely on relations between neutral (atomic and molecular) and ionized layers established for the Milky Way (see Ruzmaikin et al. 1988 for a detailed discussion and references).

The ionized layer in the Milky Way (the Reynolds (1991) layer) is several times thicker than the layer of neutral hydrogen. The exponential scale height of H I is $500\,\mathrm{pc}$ for warm diffuse hydrogen (Lockman 1984). It is plausible that the Reynolds layer is the site of dynamo activity, and then $h = 900\,\mathrm{pc}$ is the relevant scale height of the ionized layer near the Sun; this is about twice the scale height of diffuse warm H I of $500\,\mathrm{pc}$. Also the synchrotron emission forms a thick layer with an exponential scale height of about 1.8 kpc at 408 MHz (Beuermann et al. 1985). (All the scale heights mentioned refer to the galactocentric distance of the Sun of 10 kpc.)

However, M31 is different from the Milky Way. As no radio halo has been detected (Gräve et al. 1981), it probably does not have a thick ionized disc. In other galaxies these phenomena occur together, where they appear to be connected with star formation activity which is quite low in M31 (Walterbos & Braun 1994). Walterbos & Braun (1994) consider that it is possible that the Hα disc in M31 is significantly thinner than in the Milky Way, NGC 891 and NGC 4631; these authors suggest that the scale height of thermal electrons in the region of the main spiral arms of M31 (at about $10\,\mathrm{kpc}$ from the galaxy's centre) is probably smaller than $500\,\mathrm{pc}$. We consider models of M31 in which the exponential scale height of the ionized disc h is either equal to that of diffuse H I or twice as large.

In M31, the scale height of the neutral hydrogen layer $h_{\mathrm{H\,I}}$ grows with galacto-centric radius r as $h_{\mathrm{H\,I}} = 182\,\mathrm{pc} + 16(r/1\,\mathrm{kpc})$ (Braun 1991) giving 242 pc at $r = 10\,\mathrm{kpc}$; this expression describes a mixture of gas clouds and the diffuse gas.

Since the interstellar gas is collisional on the scales of interest, the steady-state strength and distribution of the large-scale magnetic field are controlled also by the total gas density (i.e., of both the neutral and ionized components) via the kinetic energy density of the interstellar turbulence. We obtained the total gas density from the surface density of H I derived by Cram et al. (1980) using the above values of $h_{\mathrm{H\,I}}$ of Braun (1991), and the CO surface densities measured by Dame et al. (1993) assuming that the scale height of molecular hydrogen is equal to $\frac{1}{2}h_{\mathrm{H\,I}}$, by analogy with the Milky Way. We used various assumptions concerning the CO to H_2 conversion factor, from the Milky Way value $X = 2.3\times10^{20}\,(\mathrm{cm^2\,K\,km\,s^{-1}})^{-1}$ as Dame et al. (1993), to a variable factor with $\log X(r) = 0.39(r/r_e - 1) + \log X_e$, where r_e is an effective radius taken equal to $7.37\,\mathrm{kpc}$, $X_e = X(r_e) = 2.4$ in units of 10^{20} cm^{-2} (K km s^{-1})$^{-1}$ and r is in kiloparsecs (see Arimoto et al. 1996). The different choices of X hardly affected our results, which are presented below for the former value of X. The midplane density profile used here

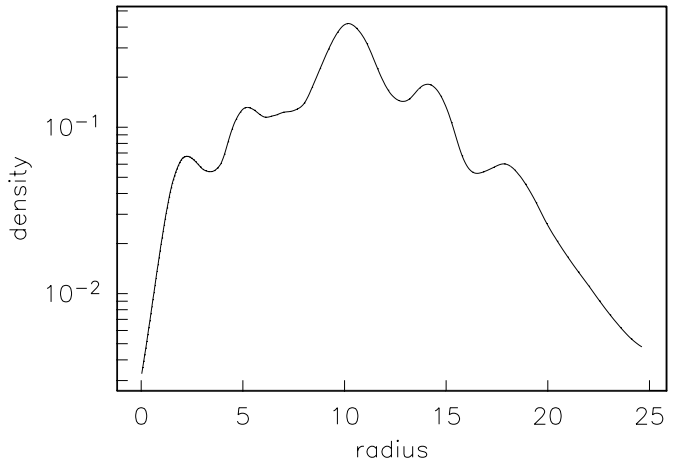

Fig. 1. The radial distribution of the total gas volume density in M31 as used, in units of the proton mass $m_p = 1.7 \times 10^{-24}\,\mathrm{g\,cm^{-3}}$. The radius is measured in kpc

is shown in Fig. 1. Besides the main gas belt at $r \simeq 10\,\mathrm{kpc}$, smaller maxima in gas density are visible at about 2.5 and $5\,\mathrm{kpc}$ radius which coincide with inner spiral arms as defined by Baade (1958).

The rotation curve of M31 was redetermined from Hα data by Kent (1989) and from H I observations by Braun (1991). We used the latter rotation curve here as it seems to account in a more consistent way for non-planar and non-circular gas motions. We note, however, that the data are rather uncertain within about $2\,\mathrm{kpc}$.

We took values of the rotational velocity of the gas from Table 3 (see also Fig. 8b) of Braun (1991), and converted them to values for the angular velocity $\Omega(r)$. These values are shown by asterisks in Fig. 2a; to avoid compression of the vertical scale we have omitted Braun's points near the galactic centre. Near the centre, the angular velocity is still rising steeply, but observations are not particularly reliable within $r \lesssim 2\,\mathrm{kpc}$, and we have made no attempt to reproduce the rotation velocities in the innermost $1\,\mathrm{kpc}$ (Boulesteix et al. 1987, Kent 1989). As we are mainly interested in processes occurring further out from the centre we, rather arbitrarily, enforced solid body rotation within $r \lesssim 2$ kpc. Two interpolations through the data points are used in this paper. The broken curve in Fig. 2a closely reproduces the continuous curve shown in Braun's Fig. 8b for $r \gtrsim 2.5$ kpc, and the continuous curve, whilst also consistent with the observed error bars, reproduces small features that are possibly present in the data. We also show the local dynamo number, $D = r(d\Omega/dr)\alpha h^3/\eta^2$, in Fig. 2b. Since D is proportional to $r\,d\Omega/dr$, apparently small differences between the two curves at $r > 2.5\,\mathrm{kpc}$ lead to significant differences in $D(r)$. The difference between the curves at $r < 2.5\,\mathrm{kpc}$ is of no physical consequence in this context.

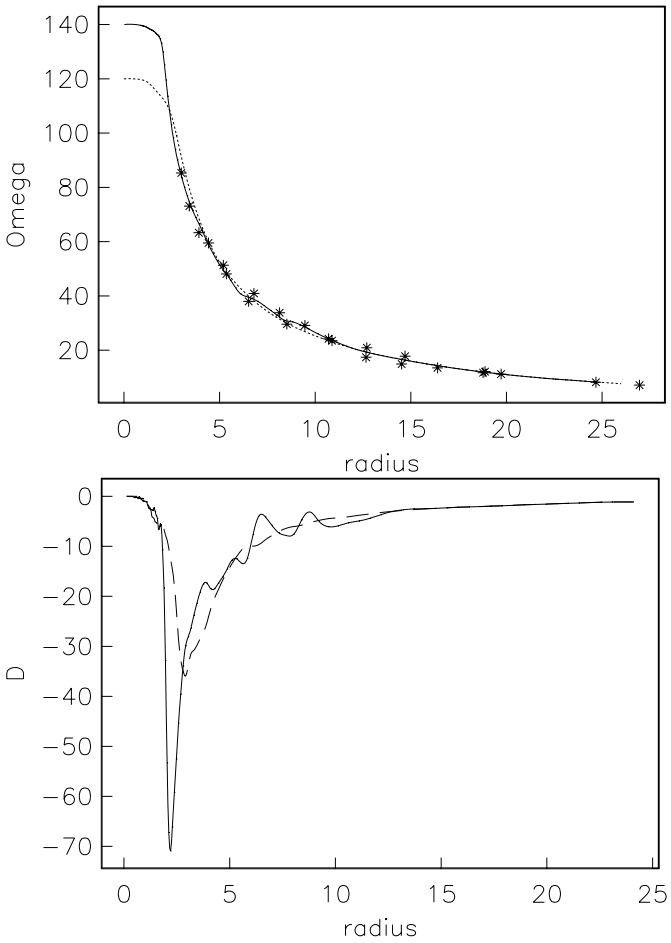

Fig. 2. **a** Rotation curves of M31 adopted in this paper (solid and broken) and the rotation curve of Braun (1991) (asterisks); **b** the local dynamo number $D(r)$ (solid and broken) for the two cases above. Units of Ω are $\mathrm{km\,s^{-1}\,kpc^{-1}}$, and the radius is measured in kpc

3. The model

In this section we first describe briefly our galactic dynamo model and then discuss its application to the particular case of M31. We solve a standard mean-field dynamo equation in the form

$$\frac{\partial \boldsymbol{B}}{\partial t} = \nabla \times (\boldsymbol{u} \times \boldsymbol{B} + \boldsymbol{u}_{\mathrm{dia}} \times \boldsymbol{B} + \alpha \boldsymbol{B} - \eta \nabla \times \boldsymbol{B}) \ , \qquad (1)$$

where $\boldsymbol{B}$ is the regular magnetic field, $\boldsymbol{u}$ is the large-scale velocity (which we assume to be purely rotational) and $\boldsymbol{u}_{\mathrm{dia}} = -\frac{1}{2}\nabla\eta$ represents the effects of turbulent diamagnetism (Vainshtein & Zeldovich 1972, Roberts & Soward 1975); α represents the alpha-effect and η is the turbulent magnetic diffusivity. We make the assumption of axisymmetry, so that $\partial/\partial\phi = 0$ when using cylindrical polar coordinates (r, ϕ, z). Our numerical code, which was originated by A. Poezd (Moscow University), has the feature that it allows the mesh spacing in the r and z directions to be very nonuniform. Thus it is possible to resolve thin galactic discs without putting an excessive number of points in a relatively passive halo region. Our simulations were carried out in a cylinder of radius R and height $2Z$. Typically we solve with $N_r \approx 110$ points distributed nonuniformly over $0 \le r \le R$, and $N_z \approx 130$ points distributed over $-Z \le z \le Z$; the minimum mesh size in (r, z) was $(50\,\mathrm{pc}, 25\,\mathrm{pc})$ and the maximum

$(500\,\mathrm{pc}, 150\,\mathrm{pc})$. Thus the disc is well resolved. For our calculations, in which the field is chosen to have strict quadrupolar parity, it is only necessary to solve Eq. (1) explicitly in $z \geq 0$. In the calculations reported here, $R \approx 24\,\mathrm{kpc}$ and $Z \approx 4\,\mathrm{kpc}$. The solution is advanced in time by a predictor-corrector method that accurately preserves the condition $\nabla \cdot \boldsymbol{B} = 0$ imposed initially. This code is described in more detail in Moss et al. (1998). Note that the α term is retained in both toroidal and poloidal equations, i.e. this is an $\alpha^2\omega$ dynamo model.

The essential ingredients of a realistic galactic dynamo model are the rotation curve $u(r) = r\Omega(r)$, the disc half-thickness h, and the equipartition field strength $B_{\mathrm{eq}} = (4\pi\rho v^2)^{1/2}$, all functions of radius. $\rho(r)$ is the total gas density averaged over z, and v is the r.m.s. turbulent velocity (assumed to be constant and equal to $10\,\mathrm{km\,s^{-1}}$). The radial density distribution shown in Fig. 1 is used to calculate $B_{\mathrm{eq}}(r)$ which is then used in Eq. (4). It is also necessary to specify the alpha coefficient α and the diffusivity η as functions of position. The lengths r and z are measured in units of kiloparsecs throughout.

We take a flared ionized disc, of half-thickness

$$h(r) = \begin{cases} h_0(1 + r/16\,\mathrm{kpc}) & \text{for } r \leq 16\,\mathrm{kpc}\,, \\ 2h_0 + 0.016(r - 16\,\mathrm{kpc}) & \text{for } r > 16\,\mathrm{kpc}\,. \end{cases} \quad (2)$$

For the standard case, $h_0 = 0.2\,\mathrm{kpc}$. The alpha coefficient is taken as

$$\alpha(r,z) = \begin{cases} C\Omega(r) f(\boldsymbol{B}) \dfrac{l^2}{h(r)} \sin \dfrac{\pi z}{1.5h(r)} & \text{for } z \leq 1.5h\,, \\ 0 & \text{for } z > 1.5h \end{cases} \quad (3)$$

(see, e.g., Ruzmaikin et al. 1988). C is an adjustable parameter of order unity and l is an estimate of the turbulent length scale in the disc, for which we assume $l = 0.1\,\mathrm{kpc}$; a precise value of l is unimportant. In order for a dynamo field to be excited, C must exceed a threshold value of about 0.4. The nonlinearity is an alpha-quenching,

$$f(\boldsymbol{B}) = \frac{1}{1 + q\boldsymbol{B}^2(\boldsymbol{r})/B_{\mathrm{eq}}^2(\boldsymbol{r})}\,, \quad (4)$$

with q an arbitrary calibration factor of order unity which can be used to adjust the calculated field strength to the observed values. (The steady state field strength in physical units then scales as $q^{-1/2}$.) Thus we have neglected any possibility of an α-effect operating outside the galactic disc (in other galaxies, regular magnetic fields possibly associated with dynamo action may occur in the galactic halo – see Sokoloff & Shukurov 1990, Beck et al. 1996 and references therein, and also Berkhuijsen et al. 1997).

Alpha-quenching is the only nonlinearity included in our model. We prefer to keep the model as simple as possible and to include only those effects which are required to reach a reasonable agreement with the available observations of M31. There are several other nonlinear mechanisms that are potentially of importance in other galaxies and/or required to explain more subtle observational effects. Some of these mechanisms, such as magnetic buoyancy, effects of the Lorentz force on the turbulent diffusivity, inflation of the galactic disc by magnetic pressure, etc. have been discussed by Schultz et al. (1994), Dobler et al. (1996), Elstner et al. (1996) and Rüdiger & Schultz (1997); a review of earlier results can be found in Beck et al. (1996).

In most runs, we neglected the vertical variation of the gas density by assuming a vertically uniform disc (thus, h defined above is the equivalent half-thickness); then the vertical distribution of $\boldsymbol{B}$ is controlled mainly by that of η and α. We also made trial runs with an exponential vertical distribution of ρ (then h is the scale height); the results differed insignificantly.

In the disc we take the magnetic diffusivity as $\eta_d = \frac{1}{3}vl$. We assume that $\eta = \eta_h \gg \eta_d$ high above the disc. At large distances from the disc, the magnetic field should become a vacuum field. For some galaxies, this transition from the disc field to a vacuum field occurs via an extended halo, and thus our procedure can be thought of as corresponding to having turbulent velocities and correlation lengths larger in the halo than in the disc (e.g. Sokoloff & Shukurov 1990, Brandenburg et al. 1992, Poezd et al. 1993). For other galaxies, such as M31, there is no well developed halo, and so our model should then be thought of as simply providing an approximation to a smooth transition to an outer vacuum region. We adopt $\eta_h = 40\eta_d$, and interpolate in $|z| > h$ by

$$\eta(r,z) = \eta_h + (\eta_d - \eta_h) \exp\left[-\left(|z| - h\right)^2 / h^2\right]\,. \quad (5)$$

We adopt, rather arbitrarily, perfectly conducting boundary conditions at $r = R$, $z = Z$, but verified that plausible changes did not significantly affect the solutions of Eq. (1) in the regions near the disc where the field is relatively strong. The key point here is that the field is concentrated far from the boundaries.

We take the seed field in the form $\boldsymbol{B} = \nabla \times \boldsymbol{A}$, where for most of our calculations

$$A_x = A_y = 0\,,\ A_z = \begin{cases} -ar^2 \exp\left(-r^2/R^2\right) & \text{for } z \leq h_0\,, \\ 0 & \text{for } z > h_0\,. \end{cases} \quad (6)$$

We also consider a seed field containing reversals

$$B_r = B_z = 0\,,\ B_\phi = \begin{cases} -ar\prod_{i=1}^{4}(r - r_i) & \text{for } z \leq h_0\,, \\ 0 & \text{for } z > h_0\,. \end{cases} \quad (7)$$

In each case, a is an arbitrary scaling factor, which we choose to give initial field strengths that are a small fraction of the equipartition values. In (7) we arbitrarily take $r_1 = 5\,\mathrm{kpc}$, $r_2 = 10\,\mathrm{kpc}$, $r_3 = 16\,\mathrm{kpc}$ and $r_4 \approx R$.

Recent simulations of magnetic field generation in accretion discs by Brandenburg et al. (1995) show that the concept of the mean-field dynamo is applicable to accretion discs, provided that the sign of the α coefficient is opposite to that assumed in the standard theory (i.e. negative rather than positive in the northern hemisphere). Such a change would lead to the dynamo number being positive rather than negative in galaxies. However, the lowest mode to be excited with a positive dynamo number is an oscillatory quadrupole mode (as, indeed, seen in the simulations of Brandenburg et al. 1995) and the critical dynamo number is then about 200 for α of the form $\alpha \propto \sin \pi z/h$, to be compared with -8 for the lowest mode with negative dynamo

number (in the local approximation for a thin disc; Ruzmaikin et al. 1980; see also Stepinski & Levy 1991, Reshetnyak et al. 1991). As this value is certainly much larger than expected for the discs of normal galaxies (except perhaps their centremost parts), we conclude that galactic dynamos would be inefficient with negative α, and the result of Brandenburg et al. (1995) is probably essentially connected with the physics involved in accretion discs, i.e. with the Balbus-Hawley instability which drives the dynamo and turbulent motions in these simulations, together with the strong rotational shear.

4. The main features of the magnetic field

Our models have field configurations in which the toroidal field strength is much greater than the poloidal. From this, we deduce that our $\alpha^2\omega$ model is operating in the $\alpha\omega$ regime. In Fig. 3a we present the field structure in the eventual steady state obtained with a somewhat supercritical $C = 0.7$ starting from a seed field of form (6), and using the rotation curve defined by the broken curve in Fig. 2a (the dynamo is excited for $C \gtrsim 0.4$). We also show the variation of toroidal field, B_ϕ, with radius near the midplane in Fig. 4. The toroidal field is strongly concentrated to the disc region, but there is only a slight indication of a magnetic belt-type structure. In particular, the strongest fields occur between 2 and $6\,\mathrm{kpc}$ radius where the radio synchrotron emission is very low (e.g. Beck & Gräve 1982). This apparent discrepancy between our models and the observed synchrotron emission will be discussed in Sect. 7.

We should reiterate that the rotation curve becomes rather unreliable within 2 kpc from the galactic centre, so we have chosen $\Omega = \text{const}$ at these radii, motivated by computational convenience (see Sect. 2). Thus magnetic features in our model near this region are not reliable.

Braun's data give a visual indication of a rising feature in the rotational velocity at around 5–7 kpc, and the continuous curve in Fig. 2a is an attempt to investigate the possible importance of this feature. With this $\Omega(r)$, we obtain the field configuration shown in Fig. 3b. Now there is a conspicuous cell-like structure, with a field minimum around $r \simeq 6$–$8\,\mathrm{kpc}$. The field maximum between 2 and $6\,\mathrm{kpc}$ radius, however, is still prominent. As is also clear from Fig. 4, the magnetic belt at approximately 8–$12\,\mathrm{kpc}$ is significantly more prominent with this version of the rotation curve. It is apparent that comparatively small changes to the rotation curve can quite markedly influence the detailed field structure. The changes we made between the broken and continuous curves in Fig. 2a we believe to be no larger than the probable errors in determining $\Omega(r)$, and so the differences between Figs. 3a and 3b are a conservative estimate of the inherent uncertainties of our (and any other) model.

As can be seen in Fig. 3c (see also Fig. 4), the magnetic belt at $r \approx 10\,\mathrm{kpc}$ is more pronounced for larger values of C, i.e., for stronger dynamo action. The value $C = 2.5$ used in this figure does not seem to be unrealistic.

We also experimented by doubling $h(r)$ (Eq. 4), keeping $C = 0.7$. The vertical scale of the magnetic field then also approximately doubled, and the field at larger radii was somewhat increased in strength relative to that at smaller radii – see Fig. 3d. This is consistent with our experience when C is increased from 0.7 to 2.5 (see above), as the local dynamo number is proportional to h^2. Thus, the effect of doubling the scale height is qualitatively similar to that of quadrupling C, except that the scale height of the field is then approximately doubled.

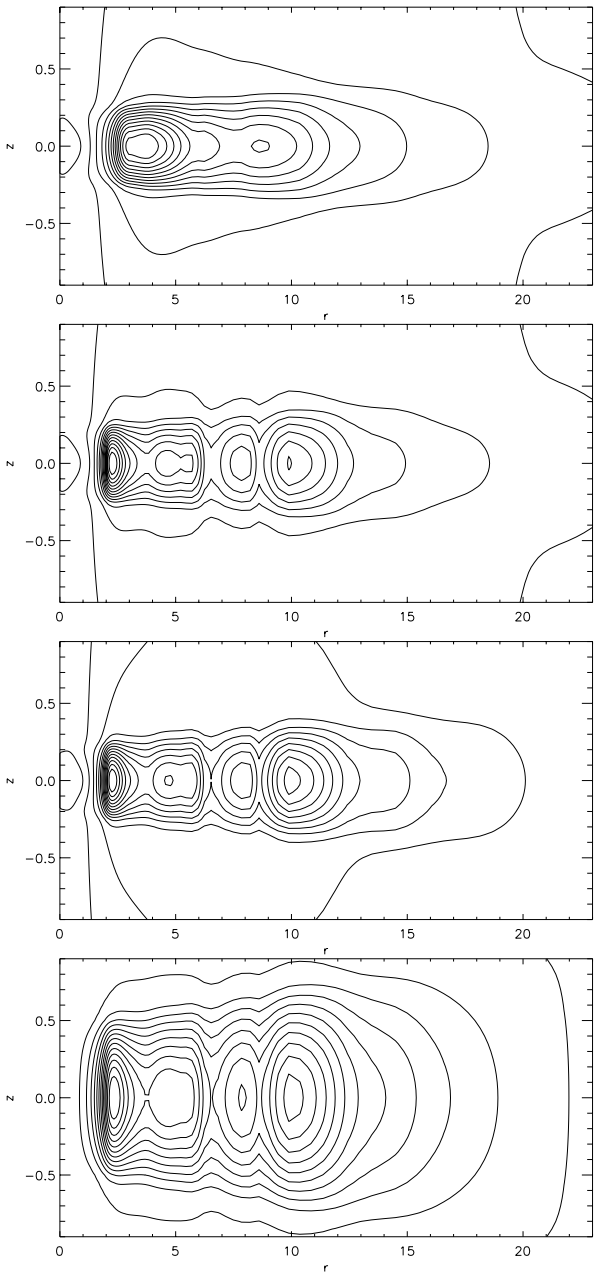

Fig. 3a–d The steady-state distributions of the large-scale toroidal magnetic field for **a** (top) the dashed rotation curve and **b** the continuous curve of Fig. 2a, both with $C = 0.7$, and **c** for the continuous curve of Fig. 2, but with $C = 2.5$. Panel **d** (bottom) gives field contours using the continuous curve, with $C = 0.7$, but with the scale height of the gas doubled. The contours are equally spaced level curves of toroidal field strength; r and z are measured in kpc

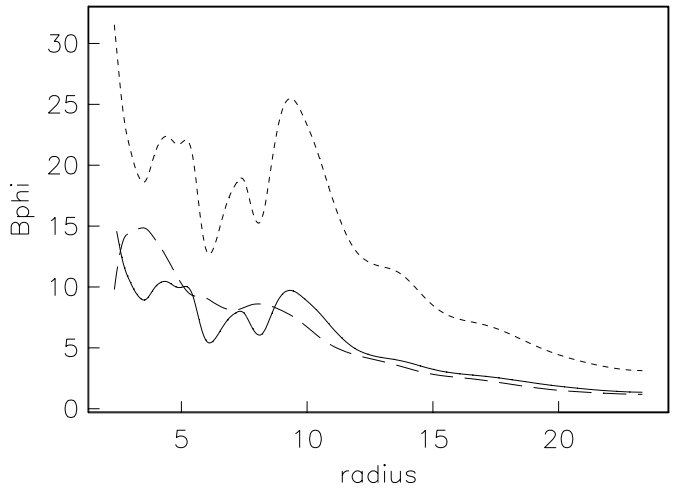

Fig. 4. The steady-state radial distributions (solid and broken curves as in Figs. 2a and b of the large-scale toroidal magnetic field strength at the midplane for the two different approximations of Braun's (1991) rotation curve, with $C = 0.7$. The distribution using the modified rotation curve and $C = 2.5$ is also shown short-dashed. The unit of field strength in the figure depends on the calibration factor q in Eq. (4), and is $0.26\,\mu$G for $q = 1/4$, bringing the values close to those observed. The radius is measured in kpc

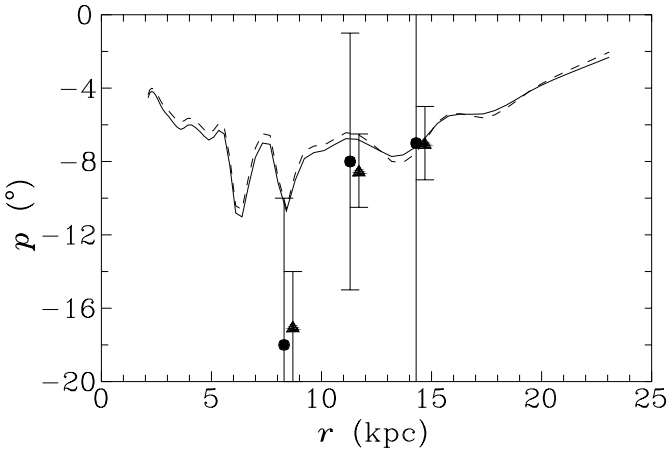

Fig. 5. The pitch angle as a function of radius for $C = 2.5$ (solid) and $C = 0.7$ (broken). Points with error bars show estimates of the pitch angles of the regular magnetic field in M31 from Beck (1982) (smaller bars) and Ruzmaikin et al. (1990) (larger bars): averages over the rings 7–10, 10–13 and 13–16 kpc are shown by filled circles, and over 7–14 kpc by the open circle

One of the most uncertain factors in mean field dynamo models is the value and spatial distribution of the α coefficient. Considering its radial variation, it appears plausible to assume that it is governed by those of Ω and h. However, its distribution perpendicular to the disc is usually taken arbitrarily, being motivated only by tradition or computational convenience (apart from fundamental symmetry properties). Fortunately, the structure of the solutions of the dynamo equations in a thin disc only weakly depends on the particular form of α as a function of z. To quantify the sensitivity of our results to the arbitrariness in the adopted distribution of α over z, we compared results obtained using Eq. (3) with those for another popular form, $\alpha \propto z/h$ for $z \le h$ and $\alpha = 0$ for $z > 1.5h$ with a linear transition between these in $h < |z| \le 1.5h$. The resulting steady field configuration is barely distinguishable from that obtained previously. We conclude that the inherent uncertainties in our dynamo model arising from the prescription of the α-effect are certainly not larger than those arising from uncertainties in the galactic rotation curves.

It can be easily understood that the steady-state magnetic field is sensitive to local features of the rotation curve, as it depends on both $\Omega(r)$ and $B_{\rm eq}(r)$. In a thin disc, a crude approximation is that the steady state field distribution is controlled locally at each radius because the radial magnetic diffusion time is significantly longer than that vertically across the disc. As a result, the steady-state radial distribution of the regular magnetic field $B_{\rm s}$ can be qualitatively determined from the requirement that the quenched value of α is equal to its critical value $\alpha_{\rm cr}$ corresponding to a marginally stable dynamo regime. For the nonlinearity (4), this yields

$$B_{\rm s} \simeq B_{\rm eq} q^{-1/2} \sqrt{D/D_{\rm cr} - 1}, \qquad (8)$$

where q is the arbitrary calibration factor from Eq. 4, $D \approx 10h^2 v^{-2} r\Omega\, d\Omega/dr$ is the local dynamo number (with $\eta = \frac{1}{3} vl$ and $\alpha = l^2\Omega/h$) and $D_{\rm cr} \simeq -10$ is its critical value corresponding to marginal excitation with $\alpha = \alpha_{\rm cr}$. In those regions where D strongly exceeds the critical value, $B_{\rm s}$ must be somewhat stronger than $B_{\rm eq}$ in order to suppress the dynamo action strongly enough to reach a steady state (usually, in galactic discs, an overshoot by a few tens of percent is sufficient). As determined by Eq. (4), the strength of the steady-state mean field scales, like $B_{\rm eq}$, as $\rho^{1/2}$.

In Fig. 5 we show the variation of pitch angle p $\left(= \tan^{-1}(B_r/B_\phi)\right)$ as a function of radius for $r \gtrsim 2\,$kpc in the disc plane for two different dynamo intensities. As in most other models of galactic dynamos and, probably, in real galaxies (see Beck et al. 1996 for a review), $|p|$ decreases with radius in the outer parts of the galaxy. Also shown in Fig. 5 are observational estimates of Beck (1982) and Ruzmaikin et al. (1990). The mean values reported by these authors are quite consistent with each other, but the errors are very different: the former paper provides lower estimates of the true errors, whereas those from the latter are upper limits. We made no attempt to include streaming velocities associated with the spiral arms; experiments of Moss et al. (1998) show that such motions tend to align instantaneously magnetic fields with the spiral arms, although if the streaming is steady over several rotation periods the situation may be more complex (Moss 1998).

To demonstrate the role of the nonlinearity (4), we made a calculation with $B_{\rm eq}^2$ independent of radius. Now the field was concentrated to the centre with a radial width of its distribution at half maximum of about $6\,$kpc, with no outer belt-like field structure. Conversely, if we remove the dependence on $\Omega(r)$ from α in Eq. (3), whilst preserving its central value, the field maximum moves to about $9\,$kpc, but the general field morphology of Fig. 3b is preserved.

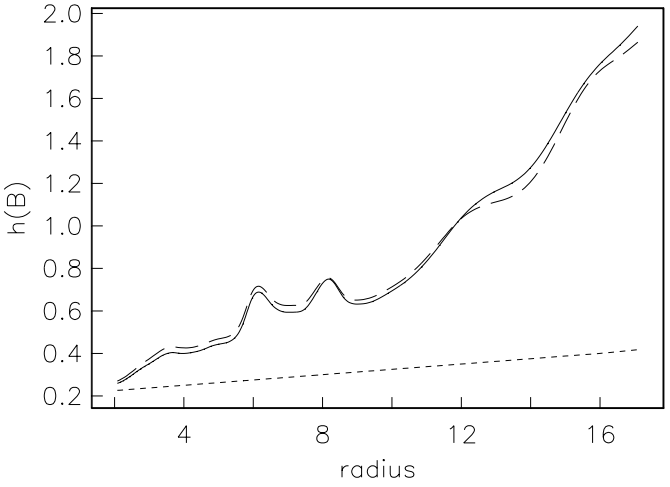

Fig. 6. The scale height of the toroidal field (found by fitting an exponential to the field values at $z = 0$ and $z = 0.2\,\mathrm{kpc}$) as a function of radius for $C = 0.7$ (solid) and $C = 2.5$ (broken); the scale height of the gas disc, Eq. (2), is also shown short-dashed

We repeated a calculation with the equipartition field strength allowed to be a function of $|z|$ also, adopting

$$\rho(r,z) = \rho_0(r)\exp\left[-|z|/h(r)\right] \ , \tag{9}$$

in our definition of $B_{\rm eq}$, where $\rho_0(r)$ is the quantity we normally refer to as $\rho(r)$. We found this had an insignificant effect on the solution, increasing the half-width of the toroidal field distribution perpendicular to the disc plane by less than 5%.

Starting with a r.m.s. value for the seed field of about 3×10^{-5} of the eventual value in the steady state (i.e. about $6 \times 10^{-11}\,\mathrm{G}$ in dimensional units), we find that after (6–7) $\times\ 10^9\,\mathrm{yr}$, the field strength has reached 70% of its value in the steady configuration, and is very close to its final geometry. This suggests a tentative lower limit on the seed field in M31 of about 10^{-11}–$10^{-10}\,\mathrm{G}$.

We also repeated the main calculation, using the continuous rotation curve of Fig. 2a, starting from the seed field given by Eq. (7). We obtained the same steady state field geometry as shown in Fig. 3b. A seed field with a sinusoidal radial dependence gave the same result. This is consistent with the conclusions of Poezd et al. (1993), that radial reversals of the toroidal magnetic field rapidly disappear in M31; the absence of reversals in the steady state is consistent with observations of M31.

We have smoothed Braun's rotation data, contaminated by observational errors of about $30\,\mathrm{km\,s^{-1}}$, to avoid excessive spurious localized features in magnetic field distribution. The final result is sensitive to the smoothing. We show in Fig. 4 the radial profiles of the steady-state magnetic field resulting from different approximations to the observed rotation curve. Here the unit of field strength is $0.26\,\mu$G, arising from our units of km/s and particles/cm^3 for turbulent velocity and density respectively and choice of $q = 1/4$. We also show the corresponding profile for our modified rotation curve with C increased to 2.5, in order to indicate the typical uncertainty associated with the choice of C and also to demonstrate that the magnetic belt becomes stronger for a stronger dynamo.

A typical difference in the rotational velocity between the two approximations is about $(10 - 20)\,\mathrm{km\,s^{-1}}$ over a radial range of about $6\,\mathrm{kpc}$. The resulting variation in magnetic field morphology is illustrated in Fig. 3a and b. This can be considered as a measure of the error in our (and any) dynamo model for the magnetic field in a galaxy associated with errors in its rotation curve. Rotation curves of more remote galaxies are known with lower accuracy than that of M31.

5. The scale height of the large-scale magnetic field

An interesting and unanticipated feature of our solutions is that the scale height of the (regular) magnetic field is significantly larger than that of the gas disc, and increases rapidly with radius – see Fig. 6. This behaviour cannot be explained by simple diffusion of the field away from the mid-plane, as then the difference between the scale heights of the field and the gas would be approximately independent of radius. A plausible explanation is that fields at large radii are primarily the result of diffusion from regions of strong generation at smaller radii. This indicates a potential importance of non-local effects in the disc dynamo of M31 (cf. Soward 1992a,b; Priklonsky et al., in prep.). The local maxima in the field scale height occur near the maxima of the field strength (see Fig. 4). Note that a doubling of the scale height of the ionized gas results in an almost uniform similar increase in the scale height of the magnetic field – see Figs. 3b,c,d. It cannot be excluded that differential rotation also contributes to the enhancement of the magnetic field outside the gas disc (we are grateful to D. Elstner for this suggestion). However we note that the rotational shear becomes weaker with radius whereas the difference between the scale heights increases.

A relatively large scale height of the regular magnetic field can have important effects on cosmic ray propagation, hydrostatic support of the gas layer, galactic winds and fountains, formation of radio halos, etc. The scale height of the total magnetic field at the solar radius in the Milky Way, derived from the scale height of the thick synchrotron disc (assuming energy equipartition or pressure balance with cosmic rays), is about 7 kpc, significantly larger than that of the gas (Beuermann et al. 1985). The synchrotron scale height is related to a mixture of the regular and random fields, so that it is difficult to say what is the 'observed' scale height of the regular field. Interpretations of Faraday rotation measures of pulsars and extragalactic sources indicate that the product $n_{\rm e}B$ (with $n_{\rm e}$ the number density of thermal electrons) has a scale height of 400–700 pc in the Milky Way (Ruzmaikin et al. 1988, p. 77; Simard-Normandin & Kronberg 1980). Then the scale height of the regular field B is 700–3000 pc assuming the scale height of thermal electrons of 900 pc (provided B has an exponential distribution with z).

We derived new estimates of the exponential scale height of the total synchrotron emission from the new 20 cm map of M31 at $45''$ resolution (Beck et al. 1998). Because of the high inclination of M31, the projected width of a spiral arm in the sky plane is determined by the vertical extent of the arm. We

took six cuts through the main belt parallel to the minor axis at $X = 25.5', 23.0'$ and $20.5'$ (5.1, 4.6 and 4.1 kpc) on the northern major axis and at $X = 14.5', 17.0'$ and $19.5'$ (2.9, 3.4 and 3.9 kpc) on the southern major axis. These cuts cross the main belt close enough to the minor axis to be almost perpendicular to the arms. We considered separately the cuts for each quadrant of the M31 image. The emission from the belt is partly resolved into emission from several individual spiral arms at this resolution. The full width at half intensity of the brightest arms was converted to exponential scale heights of synchrotron emission $h_{\rm syn}$. We obtained $h_{\rm syn} = 180 \pm 50$ pc at $r \approx 6$ kpc for the northern arms inside the belt, and 400 ± 50 pc for the brightest arms in the north at $r \approx 11$ kpc. In the south the strongest arm in the western part of the belt has $h_{\rm syn} = 320 \pm 30$ pc at $r \approx 7$ kpc, and in the eastern part $h_{\rm syn} = 500 \pm 40$ pc at $r \approx 8$ kpc. These values of r seem small because these arms are not exactly in the plane of M31, but are projected onto the belt. Both the lowest and the highest value of h_{syn} are on a bump on h_B in Fig. 6. The errors in $h_{\rm syn}$ are due to the spread in the widths obtained for the same arm identified in several cuts. The radial distances r were estimated from the spiral arm model of Braun (1991).

Assuming energy equipartition between magnetic field and the cosmic rays, we can calculate the scale heights of these two variables from $h_B = (3 + s)h_{\rm syn}$ and $h_{\rm CR} = 0.5h_B$, where $s = 0.88$ (Beck & Gräve 1982) is the spectral index of synchrotron emission. For the four cases mentioned above, we then obtain, $h_B = 700 \pm 200$ pc, 1600 ± 200 pc, 1200 ± 100 pc and 1800 ± 200 pc, respectively. These values are higher by about a factor of two than the model scale heights in Fig. 6. This could mean that the scale height of the ionized gas in M31 is twice that of HI, i.e. $h_0 \simeq 0.4$ kpc in Eq. (2) (cf. Fig. 3d). Indeed, this is the case in the solar neighbourhood as we mentioned in Sect. 2. On the other hand, h_B derived from the total synchrotron emission refers to a mixture of the regular (large-scale) and small-scale magnetic fields. If the small-scale field has a larger scale height than B, then the above estimates of h_B from synchrotron emission refer rather to the small-scale magnetic field. It is difficult to decide between these possibilities, but our model appears quite consistent with the observations in this respect.

6. Is there a central dipole?

In the main part of our investigation we considered fields of strictly quadrupolar (even) parity, as these are quite generally the more easily excited and stable fields for dynamos in discs. Moreover, fields of this parity are believed to be dominant through the major parts of spiral galaxies (e.g. Beck et al. 1996). Nevertheless, there have been suggestions that odd parity fields may be present near the centre of some spiral galaxies, and physical conditions there may be more favourable for the maintenance of dipolar fields, if the differential rotation is locally smaller.

Thus we made some experiments with initial fields consisting of a purely odd parity field in the inner region ($r \leq 5$ kpc typically) of the model, and a purely even parity field at larger radii, without restricting the parity of the solution as it evolved. We took $C = 1$. In an extreme case, the ratio of the initial energies in the even and odd parity components was 7:1. After 4 Gyr the dipole-like field was confined to within about $1\,{\rm kpc}$ of the centre, with ratio of energies of even and odd parity components of approximately 5×10^{-4}. After about 5 Gyr, the ratio was 10^{-4}, and the dipole-like component had effectively disappeared. Thus it appears unlikely that, in a conventional dynamo model such as considered here, central odd parity fields can persist.

We note that Donner & Brandenburg (1990), using a linear dynamo model, found that a central dipole-like magnetic field might sometimes be excited. This result appears not to survive in the non-linear regime. Note, however, that Elstner et al. (1996) obtained oscillatory dipole solutions in their models of galactic dynamos when using a model of turbulence from Rüdiger & Kitchatinov (1993). These dipole solutions occur when the correlation time of the interstellar turbulence exceeds the nominal value of 3×10^7 years by a factor of 5.

7. Discussion and conclusions

Our model successfully reproduces the observed magnetic belt, which is a relatively robust feature of the nonlinear dynamo models for M31. The detailed radial dependence of the steady-state field strength (Fig. 4) shows a close correspondence to the radial profile of the local dynamo number shown in Fig. 2b. This correspondence is explained by Eq. (8); it is especially strong for a slightly supercritical dynamo, that is for $D/D_{\rm cr} \simeq 1$.

Not all the features of the calculated radial profile of B correspond to those so far observed. For example, the radio synchrotron emission has a minimum at $r = 3$–$5\,{\rm kpc}$. On the assumption of energy equipartition between cosmic rays and magnetic fields, this would suggest a field minimum around this location, whereas the calculated field has, quite robustly, a local maximum at about this radius.

Specific features of the models as well as intrinsic properties of M31 could explain this discrepancy. Fig. 6 shows that the relative height of the maximum near 4 kpc decreases when C increases, so that the maximum is less pronounced if the dynamo is stronger than assumed. The maximum is significantly suppressed even for a moderately supercritical value of $C = 2.5$, or by increasing uniformly the scale height of the gas (compare Figs 3b,c,d).

Furthermore, this local maximum near $r = 4\,{\rm kpc}$ could be an artifact of an imprecise rotation curve. As we mentioned above, the variations of rotational velocities of 10–$20\,{\rm km\,s^{-1}}$ can significantly affect the ratio of the field strengths at $r \approx 4\,{\rm kpc}$ and $10\,{\rm kpc}$ – see Figs 3 and 4. Using Eq. (8), we find that the variation of the rotation velocity Δu, required to produce a variation $\Delta B_{\rm s}$ in the steady-state field strength over a radial range Δr is given by

$$\frac{\Delta u}{u} \simeq \frac{B_{\rm s}\Delta B_{\rm s}}{2\pi\rho V^2}\,\frac{r\Delta r}{h^2}\ .$$

Thus, a variation of $\Delta u/u \simeq 0.14$, or $\Delta u \simeq 30\,{\rm km\,s^{-1}}$ would be sufficient to eliminate completely the local field maximum at $r \approx 4\,{\rm kpc}$, where we took $B_{\rm s} = 1.3\,\mu{\rm G}$, $\Delta B_{\rm s} = 1\,\mu{\rm G}$,

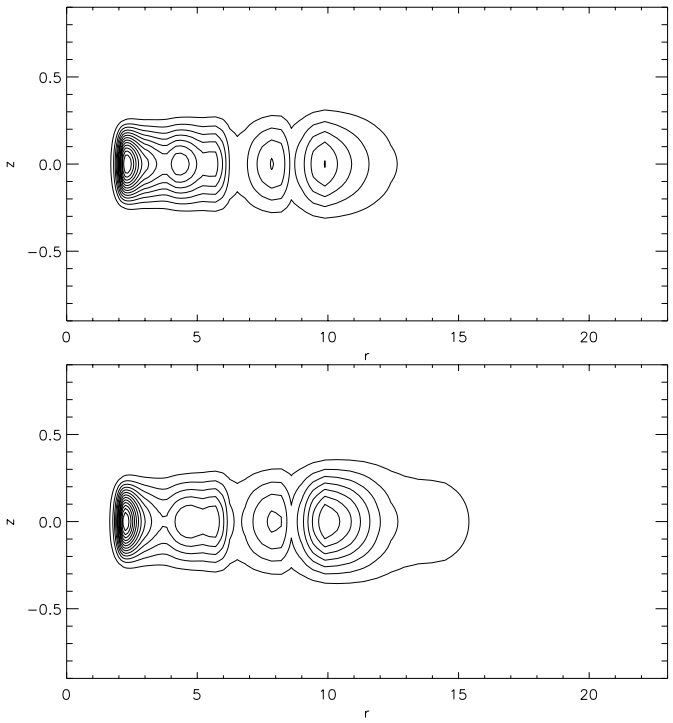

Fig. 7. Equally spaced contours of B^2 for **a** $C = 0.7$ and **b** $C = 2.5$. Note the better defined outer belt for the stronger dynamo. r and z are measured in kpc

$\rho = 1.7 \times 10^{-25}\,\mathrm{g\,cm^{-3}}$, $u = 240\,\mathrm{km\,s^{-1}}$, $r = 4\,\mathrm{kpc}$, $\Delta r = 1\,\mathrm{kpc}$ and $h = 0.25\,\mathrm{kpc}$. Clearly, this amount of variation is well within the accuracy of the rotation curve and we conclude that the maximum at $r \approx 4\,\mathrm{kpc}$ can be an artifact of the badly known kinematics of M31.

There are other possibilities that might remove the field maximum at $r \simeq 4$–$5\,\mathrm{kpc}$. For example, the gas in this region may have physical properties different from that in the main belt, so that the α-effect may operate differently there, with the dynamo generating weaker fields. However, it is impossible now to assess these uncertainties, because the detailed physics of the α-effect is not yet understood.

On the other hand, it cannot be excluded that there really is an inner belt of field, as suggested by our computations, which has so far escaped detection. We show in Fig. 7 level lines of the magnetic field squared projected on to a meridian plane; the synchrotron intensity is presumably proportional to this quantity. As expected, B^2 exhibits both a better defined outer belt and a weaker secondary maximum at $r \approx 4 - 5\,\mathrm{kpc}$. This local maximum in B could well occur in the real galaxy, but not be detected because of a lack of cosmic-ray electrons. With a propagation velocity equal to the Alfvén velocity, approximately $10\,\mathrm{km\,s^{-1}}$, cosmic rays from the main belt could propagate only over a distance of $1\,\mathrm{kpc}$ in $10^8\,\mathrm{yr}$, the cosmic ray confinement time. Thus, only cosmic rays generated close to $r = 4\,\mathrm{kpc}$ are available to illuminate the possible maximum of magnetic field there.

There are several spiral arms in M31 located at about $r = 4\,\mathrm{kpc}$ (at different azimuthal angles). They are visible as relative maxima in radial profiles in the gas density (Fig. 1), H_α (Devereux et al. 1994), the number surface density of massive stars (Berkhuijsen & Humphreys 1989) and other constituents. Fig. 12 of the latter paper shows that the surface density of massive stars, and thus the number of supernova remnants thought to generate cosmic rays, near $r = 4\,\mathrm{kpc}$ is about a factor of 7 lower than within the belt. As the synchrotron intensity at $\lambda 20\,\mathrm{cm}$ (Beck et al. 1998) at this position is only lower by a factor of 3.8, it follows that the total magnetic field strength at this radius is higher by a factor 1.4. The corresponding ratio for the regular field strengths in Fig. 6 (with $C = 2.5$) is 1.1 at $r \approx 4\,\mathrm{kpc}$, even lower than estimated from the observations. Hence the high field strength near this radius obtained from our model could well be real. In this case, energy equipartition between cosmic rays and magnetic fields does not hold in the inner arms, possibly because of a lack of cosmic-ray production around these radii.

Further searches for magnetic field inside $r \simeq 8\,\mathrm{kpc}$ should concentrate on the Faraday effect. We predict a regular field strength of at least $2.5\,\mu\mathrm{G}$ around $r = 4\,\mathrm{kpc}$. The gas density there is approximately 5 times lower than in the main belt at $r = 10\,\mathrm{kpc}$, and we may assume the same factor for the ionized gas density, leading to $n \simeq 0.005\,\mathrm{cm^{-3}}$ for the ionized gas. The resulting Faraday rotation measure is $1.6 n B_\parallel h \tan i \approx 40\,\mathrm{rad\,m^{-2}}$ for $h = 400\,\mathrm{pc}$, where $i = 78°$ is the inclination angle. Such values are detectable in sufficiently strong, linearly polarized radio sources behind M31. Two out of three suitable sources observed by Han et al. (1998) indicate a significant magnetic field at about $r = 5\,\mathrm{kpc}$. A firm confirmation would need new, more sensitive observations.

One notable defect of our model is the absence of any streaming motions associated with the spiral pattern. If these motions are concentrated to the region of the observed magnetic belt, this might improve the correspondence between the model and the observed fields. In particular, inclusion of such streaming motions might be expected to improve the agreement between the observed and calculated pitch angles, and perhaps to reduce the necessity for tuning the representation of the rotation curve.

In conclusion, we have shown that the earlier explanation of the magnetic ring in M31 is unsatisfactory, not only because the rotation curve used earlier has been significantly revised, but also because that work underestimated the interaction between eigenfunctions localized in different regions. The latter point, which is perhaps of lesser importance for the current application, is developed by Moss et al. (1998). Our model includes recent determinations of the relevant physical parameters, the rotation curve and radial variation of gas density. We do obtain an extended belt of field at $r \approx 7$–$12\,\mathrm{kpc}$, more-or-less in accordance with observations. We find evidence of another maximum of the large-scale magnetic field near $r = 4\,\mathrm{kpc}$. This can be reconciled with observations of synchrotron emission if there is no equipartition between magnetic fields and cosmic rays at that radius.

An interesting feature of our results is the relatively large scale-height of the magnetic field compared to that of the gas.

As discussed in Sect. 5, if the result is generic for spiral galaxies, then it may have quite far-reaching effects on dynamical models for these galaxies. In particular, a thick layer of horizontal regular magnetic field can confine cosmic ray particles efficiently, hamper gas outflows from the disc and affect the hydrostatic equilibrium of the interstellar gas.

Acknowledgements. The numerical code used in this paper was originated by A.D. Poezd. This work was supported by PPARC, NATO Collaborative Research Grant CRG1530959, grants 96-02-016252 and 96-02-00094G from the Russian Foundation for Basic Research and the Deutsches Forschungsgemeinschaft, and ECHCM contract ERBCHRXCT940483. We are grateful to the referee, D. Elstner, for useful comments. D.S. acknowledges partial financial support from the Royal Society and the University of Newcastle.

References

Arimoto N., Sofue Y., Tsujimoto T., 1996, PASJ 48, 275
Baryshnikova Y., Ruzmaikin A., Sokoloff D.D., Shukurov A., 1987, A&A 177, 27
Baade W., 1958, Specola Astron. Vatic. 5, 1
Beck R., 1982, A&A 106, 121
Beck R., Gräve R., 1982, A&A 105, 192
Beck R., Berkhuijsen E.M., Wielebinski R., 1980, Nat 283, 272
Beck R., Loiseau N., Hummel E. et al., 1989, A&A 222, 58
Beck R., Brandenburg A., Moss D., Shukurov A., Sokoloff D., 1996, ARAA 34, 155
Beck, R., Berkhuijsen, E.M., Hoernes, P., 1998, A&A, in press
Berkhuijsen E.M., 1977, A&A, 57, 9
Berkhuijsen E.M., Humphreys R.M., 1989, A&A 214, 68
Berkhuijsen E.M., Wielebinski R., Beck R., 1983, A&A 117, 141
Berkhuijsen E.M., Horellou C., Krause M. et al., 1997, A&A 318, 700
Beuermann K., Kanbach G., Berkhuijsen E.M., 1985, A&A 153, 17
Boulesteix J., Georgelin Y.P., Lecoarer E., Marcelin M., Monnet G., 1987, A&A 178,91
Brandenburg, A., Donner, K.J., Moss, D., Shukurov, A., Sokoloff, D.D., 1992, A&A 259,453
Brandenburg A., Nordlund Å., Stein R.F., Torkelsson U., 1995, ApJ 446, 741
Braun R., 1991, ApJ 372, 54, 1991
Brinks E., Shane W.W., 1984, A&AS 55, 1979
Cram T.R., Roberts M.S., Whitehurst R.N., 1980, A&AS 40, 215
Dame T.M., Koper E., Israel F.P., Thaddeus P., 1993, ApJ 418, 730
Deharveng J.M., Pellet A., 1975, A&A 38, 15
Dettmar R.-J., 1992, Fund. Cosm. Phys. 15, 143
Devereux N.A., Price R., Wells L.A., Duric N., 1994, AJ 108, 1667
Dobler W., Poezd A.D., Shukurov A., 1996, A&A 312, 663
Donner, K.J., Brandenburg, A., 1990, A&A 240,289
Elstner D., Rüdiger G., Schultz M., 1996, A&A 306, 740
Gräve R., Emerson D.T., Wielebinski R., 1981, A&A 98, 260
Han J.L., Beck R., Berkhuijsen E.M., 1998, submitted to A&A
Haud U., 1981, Astrophys. Sp. Sci. 76, 477
Kent S.M., 1989, AJ 97, 1614
Krasheninnikova Y., Ruzmaikin A., Sokoloff D., Shukurov A., 1989, A&A 213, 19
Lockman F.J., 1984, ApJ 283, 390
Moss, D., 1998, to appear in MNRAS
Moss D., Korpi M., Rautiainen P., Salo H., 1998, A&A 329,895
Moss, D., Shukurov, A., Sokoloff, D.D., 1998, submitted to Geophys. Astrophys. Fluid Dyn.
Poezd A., Shukurov A., Sokoloff D., 1993, MNRAS 264, 285
Pooley G.G., 1969, MNRAS 144, 101
Reshetnyak M.Yu., Sokoloff D.D., Shukurov A., 1991, Magnetohydrodynamics 28, 224
Reynolds R.J., 1991, in Proc IAU Symp. 144, The Interstellar Disk-Halo Connection in Galaxies, ed. H. Bloemen, Kluwer, Dordrecht, p. 67
Roberts M.S., Whitehurst R.N., 1975, ApJ 201, 327
Roberts P.H., Soward A.M., 1975, Astron. Nachr. 296, 49
Rubin V.C., Ford W.K., 1970, ApJ 159, 379
Rüdiger G., Kitchatinov, L.L., 1993, A&A 269, 581
Rüdiger G., Schultz M., 1997, A&A, 319, 781
Ruzmaikin A.A., Shukurov A.M., 1981, Sov. Astron. 25, 553
Ruzmaikin A.A., Sokoloff D.D., Turchaninov V.I., 1980, Sov. Astron. 24, 182
Ruzmaikin A.A., Sokoloff D.D., Shukurov A.M., 1985, A&A 148, 335
Ruzmaikin A.A., Shukurov A.M., Sokoloff D.D., 1988, Magnetic Fields of Galaxies, Kluwer, Dordrecht
Ruzmaikin A., Sokoloff D.D., Shukurov A., Beck R., 1990, A&A 230, 284
Schultz M., Elstner D., Rüdiger G., 1994, A&A 286, 72
Simard-Normandin M., Kronberg P.P., 1980, ApJ 242, 74
Sokoloff, D.D., Shukurov, A.M., 1990, Nat. 347, 51
Soward A.M., 1992a, Geophys. Astrophys. Fluid Dyn. 64, 163
Soward A.M., 1992b, Geophys. Astrophys. Fluid Dyn. 64, 201
Stepinski T.F., Levy E.H., 1991, ApJ 379, 343
Vainshtein S.I., Zeldovich Ya.B., 1972, Usp. Fiz. Nauk 106, 431 (Sov. Phys. Usp. 15, 159)
Walterbos R.A.M., Braun R., 1994, ApJ 431, 156
Xu C., Helou G., 1994, ApJ 426, 109
Xu C., Helou G., 1996, ApJ 456, 152
Zeldovich Ya.B., Ruzmaikin A.A., Sokoloff D.D., 1983, Magnetic Fields in Astrophysics, Gordon and Breach, New York